



Biophysical effects on the interannual variation in carbon dioxide exchange of an alpine meadow on the Tibetan Plateau

Lei Wang¹, Huizhi Liu¹, Jihua Sun², and Yaping Shao³

5 1 LAPC, Institute of Atmospheric Physics, Chinese Academy of Sciences, Beijing 100029, China

2 Meteorological Observatory of Yunnan Province, Kunming 650034, China

3 Institute for Geophysics and Meteorology, University of Cologne, Cologne, 50937, Germany

Correspondence to: Huizhi Liu (huizhil@mail.iap.ac.cn)

10 **Abstract.** Eddy covariance measurements from 2012 to 2015 were used to investigate the interannual
variation in carbon dioxide exchange and its control over an alpine meadow on the southeast margin of the
Tibetan Plateau. The annual net ecosystem exchange (NEE) from 2012 to 2015 was -114.2, -158.5, -159.9
and -212.6 g C m⁻² yr⁻¹ and generally decreased with the mean annual air temperature (MAT). An exception
occurred in 2014, which had the highest MAT. This was attributed to higher ecosystem respiration (RE) and
15 similar gross primary production (GPP) in 2014 because the GPP increased with MAT but became saturated
due to the photosynthesis capacity limit. In the spring (March to May) of 2012, lower air temperature (T_a)
and drought events delayed grass germination and reduced GPP. In the late wet season (September to October)
of 2012 and 2013, the lower T_a in September and its negative effects on vegetation growth caused earlier
grass senescence and significantly lower GPP. This indicates that the seasonal pattern of T_a greatly affected
20 the annual total GPP, which is consistent with the result of the homogeneity-of-slopes model. The model
shows that the climatic seasonal variation explained 48.6% of the GPP variability, and the percentage of
climatic interannual variation and the ecosystem functional change were 9.7% and 10.6%, respectively.

Keyword: Carbon dioxide exchange; Interannual variation; Alpine meadow; Tibetan Plateau

25



1 Introduction

In the last decade, the carbon dioxide exchange in grassland ecosystems has attracted much attention (Aires et al., 2008; Baldocchi, 2008; Hunt et al., 2004; Suyker et al., 2003) because grasslands cover 32% of the global land surfaces and may contribute greatly to the carbon cycle on a global scale (Parton et al., 1995).

30 The annual total net ecosystem exchange (NEE) for grasslands has a large range from $-650 \text{ g C m}^{-2} \text{ year}^{-1}$ to $160 \text{ g C m}^{-2} \text{ year}^{-1}$ due to climate variability and land use changes (Gilmanov et al., 2007; Wang et al., 2016a). The climatic factors of CO_2 exchange also vary under various climate conditions (Du and Liu, 2013; Fu et al., 2009; Xu and Baldocchi, 2004). Most of previous studies focused on the low-lying grasslands (Gilmanov et al., 2010).

35 The alpine meadow in China is the primary grassland type of the nation and is mainly distributed in the Qinghai-Tibetan plateau (DAHV and CISNR, 1996; Liu et al., 2008). The warming trend in high-altitude areas has been observed to be more pronounced, such as the Tibetan Plateau and its southeast margin (Fan et al., 2011; Liu and Chen, 2000). Several studies of CO_2 exchange on the Qinghai-Tibetan plateau have been performed, where the mean annual T_a is approximately 0°C (Gu et al., 2003; Kato et al., 2006; Shi et al., 2006; 40 Zhao et al., 2006). The daily CO_2 fluxes of the alpine meadow-steppe in Damxung, Tibet were jointly affected by air temperature and soil moisture (Fu et al., 2009), while the daily CO_2 fluxes of an alpine shrubland at Haibei, Qinghai were sensitive to air temperature (Zhao et al., 2006). On an annual scale, the measurements at the Haibei alpine meadow revealed that the annual CO_2 uptake was increased by the earlier onset of the growing season, which was caused by higher air temperature (Kato et al., 2006). The Lijiang 45 alpine meadow is in a much warmer area (the mean annual T_a is 12.7°C). A spring drought event and relatively low soil moisture significantly delayed the start time of grass germination and reduced the annual CO_2 uptake (Wang et al., 2016b). How the annual CO_2 exchange responds to the mean annual air temperature (global warming) has not been clear for the alpine meadow ecosystems.

As previous studies proposed, year-to-year changes in CO_2 exchange are attributed to climatic variability 50 (Hui et al., 2003; Xu and Baldocchi, 2004). Fluxes may directly respond to climatic drivers or be indirectly affected by the functional changes or the changes in the flux-climate relationships (Polley et al., 2008). Statistic models have been used to partition the interannual variation (IAV) of the CO_2 exchange (Hui et al., 2003; Richardson et al., 2007; Teklemariam et al., 2010). For example, Shao et al. (2014) found that 77% of the observed variation in NEE was explained by functional changes in the moist grassland in USA, while 55 variations of climatic variables could better explain the IAV of NEE for a meadow in Denmark and (Jensen et al., 2017) and mixed-grass prairies in the semiarid area of USA (Polley et al., 2008). The relative importance of the direct and indirect effects of the climatic variables on the interannual variations in CO_2 exchange for the alpine meadow in China has not been quantified.

The CO_2 exchange between the atmosphere and the Lijiang alpine meadow was measured using eddy



60 covariance technique from 2012 to 2015. The objectives of this study include: (1) to examine the seasonal
and interannual variation in NEE, GPP, RE and the parameters of ecosystem photosynthesis and respiration;
(2) to investigate the main environmental controls of the total GPP, RE and NEE on the seasonal and annual
scales; and (3) to partition the interannual variation in GPP, RE and NEE into climatic variability and
vegetation growth.

65

2 Observation site and methods

2.1 Observation site

The observation site (27°10'N, 100°14'E, 3560 m a.s.l.) is located at Maoniuping of Yulong Snow
Mountain to the north of Lijiang City on the Tibetan Plateau, China. The study area is under the plateau
70 monsoon climate, which is influenced by the southwest and southeast monsoons. The wet and dry seasons are
clear, and the wet season is from June to October. The 30-year mean annual total precipitation (1981-2010) at
Lijiang City (2400 m a.s.l.) is 980.3 mm, and 85% of the precipitation is concentrated in the wet season. The
30-year MAT is 12.6°C (data from the Lijiang Meteorology Bureau). The dominate species of this alpine
meadow are *Kobresia Willd* grass, with a maximum height of 20 cm, and *Berberis Linn* shrub, with a
75 maximum height of more than 60 cm. The surface is covered by green vegetation, litter and bare soil. The
soil type is loamy soil with a dark brown color, which has lower reflectance than the grass canopy (Guo et al.,
2009).

2.2 Field measurements and normalized difference vegetation index (NDVI)

80 The eddy covariance (EC) system was used to measure 3-D wind speed and the H₂O and CO₂
concentrations at a height of 2.5 m with 10 Hz frequency. The system consists of a three-dimensional sonic
anemometer (CSAT3, Campbell, USA) and an open-path CO₂/H₂O infrared gas analyzer (LI-7500A, LI-COR,
USA). The low response measurements (1/3 Hz frequency) performed in this study include air temperature
and relative humidity at a height of 2.5 m close to the EC system (HMP45C, Campbell, USA). Net radiation
85 (including shortwave and longwave radiation, CNR4, Kipp&Zonen, Netherlands) and photosynthetic active
radiation (LI190SB, LI-COR, USA) were measured at 1.5 m. Soil temperature (109-L, Campbell, USA) and
soil water content (CS616, Campbell, USA) were measured at a depth of 5 cm below the ground. The
precipitation (including solid precipitation in the winter) was measured using a weighing bucket precipitation
gauge (T-200B, Geonor, Norway). All measurements were controlled by a data logger (CR3000, Campbell
90 Scientific, USA), and the data were stored on a 2-GB CF card.

Four points around the flux tower were selected to investigate the variations in vegetation growth. The
250×250 m² gridded NDVI data at 16-day intervals (product name: MOD13Q1) for the four points were
obtained from the Moderate Resolution Imaging Spectrometer (MODIS) on the EOS-1Terra satellite and



were averaged to represent the meadow in this observation site.

95

2.3 Flux calculation and quality control

EddyPro software (version 5.1, LI-COR, USA) was used to calculate the half-hourly CO₂ flux based on the 10 Hz raw data. After a spike detection (Vickers and Mahrt, 1997), the sector-wise planar fit method was used to transform the coordinate system due to a terrain slope of approximately 10° (Wilczak et al., 2001).
100 Other corrections for CO₂ flux include spectral loss correction (Moore 1996,) and density correction (WPL correction) (Webb et al., 1980).

Stationary and integral turbulence characteristics tests were used for flux quality control (Foken and Wichura, 1996). When u* was less than 0.1 m s⁻¹, the CO₂ flux was dependent on u* and was discarded. Since there is a coniferous forest approximately 350 m to the north of the site, an analytical footprint model
105 was used to determine whether the half-hourly CO₂ flux is influenced by the forest and needs to be removed (Kormann and Meixner, 2001).

After quality control, approximately 70% of the CO₂ fluxes were subjected to further analysis. Linear interpolation was used to fill the flux gaps of less than 2 hours. To fill gaps longer than 2 hours, marginal distribution sampling, an improved 'look up table' method, was used (Falge et al., 2001; Lloyd and Taylor,
110 1994)

2.4 Data analysis

The relationship between daytime NEE (NEE_{daytime}) and PAR was described by the Michaelis-Menten model (Falge et al., 2001):

$$115 \quad NEE_{daytime} = \frac{\alpha NEE_{sat} PAR}{\alpha PAR + NEE_{sat}} + RE_{bulk} \quad (1)$$

where NEE_{sat} is the NEE at the saturated light level, α is the apparent quantum yield ($\mu\text{mol CO}_2 \mu\text{mol}^{-1}$ photons) and RE_{bulk} is the bulk estimated RE.

The Van't Hoff equation was used to evaluate the relationship between the nighttime NEE (NEE_{nighttime}, $\mu\text{mol CO}_2 \text{ m}^{-2} \text{ s}^{-1}$) and soil temperature at a depth of 5 cm (T_s, °C) (Aires et al., 2008):

$$120 \quad NEE_{nighttime} = a \exp(bT_s) \quad (2)$$

where a and b are the regression parameters. The temperature sensitivity coefficient (Q₁₀) of RE was determined using the following equation.

$$Q_{10} = \exp(10b) \quad (3)$$

The partitioning of NEE into GPP and RE was based on the assumption that the sensitivity of RE to soil
125 temperature was the same during the day and at night (Falge et al., 2001). The regression parameters derived



from the nighttime data were extrapolated to the daytime to calculate the daytime RE and the daily RE. The daily GPP was calculated as follows.

$$GPP = RE - NEE \quad (4)$$

130 3 Results

3.1 Weather conditions and NDVI

The daily integrated solar radiation (S_{in}) varied from 1.15 to 32.40 MJ m⁻² d⁻¹ (Figure 1a). The mean S_{in} in spring (March to May) was 17.0 to 19.93 MJ m⁻² d⁻¹ and was obviously larger than those in other season. In the wet season, the mean S_{in} was 9.99 to 11.05 MJ m⁻² d⁻¹.

135 The mean annual air temperature (T_a) was 5.92 to 6.32°C (Table 1). The daily mean T_a ranged from 0.41 to 14.96°C in the wet season and decreased to the minimum value of -9.06°C in the winter. In contrast, the soil temperature never decreased below 0°C, and the maximum value was 16.48°C (Figure 1b). The vapor pressure deficit (VPD) reached its maximum value of 1.07 kPa before the wet season (Figure 1c). The VPD decreased to near 0 kPa, and the mean VPD for the wet season was 0.125 to 0.166 kPa.

140 The annual precipitation from 2012 to 2015 ranged from 1066.1 to 1257.4 mm. The precipitation for the wet season ranged from 906.1 to 1092.6 mm, accounting for 85% to 91% of the annual total precipitation (Table 1). The mean annual soil water content (SWC) had small interannual variability, from 0.227 to 0.233 m³ m⁻³. In the wet season, SWC reached its maximum value of approximately 0.35 m³ m⁻³, and the minimum SWC was 0.15 m³ m⁻³ (Figure 1d).

145 The NDVI for this alpine meadow showed clear seasonal and interannual variation (Figure 1e). The NDVI exceeded 0.4 at the end of April or late May, depending on the amount and distribution of precipitation in the spring (March to May). The maximum NDVI for each year was 0.72 (2013) to 0.60 (2012). In all four years, NDVI decreased below 0.4 at the end of October.

150 3.2 Seasonal and interannual variations in NEE_{sat} , α and Q_{10}

The daytime NEE and PAR were averaged with the PAR bins of 100 $\mu\text{mol m}^{-2} \text{s}^{-1}$ to avoid random errors. For each month in the wet season, the daytime NEE decreased with PAR until reaching a critical PAR. Above the critical PAR, the daytime NEE increased and the CO₂ uptake was depressed (Figure 2a). To derive NEE_{sat} and α , the NEE and PAR data were used only when PAR was below the critical value. NEE_{sat} showed clear seasonal variation (Table 2). The mean NEE_{sat} values for each month show that NEE_{sat} increased starting in June (-11.59 $\mu\text{mol m}^{-2} \text{s}^{-1}$) and reached its maximum value in August (-20.14 $\mu\text{mol m}^{-2} \text{s}^{-1}$). The highest NEE_{sat} during the whole observation period occurred in August of 2014 (-23.75 $\mu\text{mol m}^{-2} \text{s}^{-1}$). NEE_{sat} then declined with grass senescence in September and October. The NEE_{sat} in October (-9.36 $\mu\text{mol m}^{-2} \text{s}^{-1}$) was



less than half that in August. The interannual variations in NEE_{sat} was also large. For example, NEE_{sat} in
160 September 2015 ($-21.44 \mu\text{mol m}^{-2} \text{s}^{-1}$) was almost twice that in September 2013 ($-11.43 \mu\text{mol m}^{-2} \text{s}^{-1}$; Table 2).
On the monthly scale, 81% of the variation in NEE_{sat} can be explained by the mean NDVI (Figure 2b). Over
this meadow, NEE_{sat} did not correlate with SWC significantly because the soil water conditions were always
good in the wet season.

At monthly intervals, there were large random errors in the regression between RE and T_{soil} . For example,
165 the R^2 for each month of the wet season in 2012 was 0.04 to 0.12. Thus, in 2012, the data in the wet and dry
season were combined to fit the regression (Figure 3a). The Q_{10} in the wet seasons was similar,
approximately 3.45 (Table 3), which was in the normal range of previous studies (1.2 to 3.7; Falge et al.,
2001). These values were obviously higher than those for temperate grasslands (1.99 to 3.07; Wang et al.,
2016a), Mediterranean grasslands (1.22 to 2.36; Airst et al., 2008) and the Haibei alpine meadow (1.50 to
170 2.27; Kato et al., 2004). Q_{10} was obviously lower in the dry season than in the wet season.

3.3 Seasonal and interannual variation in NEE, GPP and RE

The ecosystem started to absorb CO_2 (negative value of NEE) on DOY 165 in 2012, DOY 137 in 2013,
DOY 116 in 2014, and DOY 104 in 2015; then, NEE decreased (Figure 4). The minimum daily NEE for each
175 year occurred in July or August ($-3.52 \text{ g C m}^{-2} \text{ d}^{-1}$ on DOY 196 in 2012, $-3.35 \text{ g C m}^{-2} \text{ d}^{-1}$ on DOY 218 in
2013, $-3.43 \text{ g C m}^{-2} \text{ d}^{-1}$ on DOY 243 in 2014, and $-4.16 \text{ g C m}^{-2} \text{ d}^{-1}$ on DOY 210 in 2015). NEE increased
significantly starting in September and became positive on DOY 293 in 2012, DOY 305 in 2013, DOY 295 in
2014 and DOY 297 in 2015. The maximum difference in the start time of CO_2 uptake was 61 days while the
difference in the end time was 12 days. The CO_2 uptake period was much shorter in 2012 (129 days) than in
180 2013 (169 days), 2014 (180 days) and 2015 (194 days).

The daily GPP increase started earlier than CO_2 uptake. The seasonal pattern in daily GPP was similar to
that of NEE, and the amplitude of GPP was larger than that of NEE. The maximum daily GPP for each year
was 6.02, 5.47, 6.23 and 5.95 $\text{g C m}^{-2} \text{ d}^{-1}$ from 2012 to 2015. Compared with the NEE and GPP, the seasonal
variation in RE was smaller during the wet season. In particular, RE varied slightly from June to August.

185 The annual GPP in 2014 and 2015 was obviously higher than in 2012 and 2013 due to the larger NDVI
(Figure 5; Table 1, 4). In contrast, RE was highest in 2014 among the four years because it had similar Q_{10}
but the highest air temperature (Table 1). Therefore, the annual NEE in 2014 was similar to that in 2013 but
lower than that in 2015, although the GPP was similar in 2014 and 2015. The spring drought produced a
significantly lower NDVI in 2012; consequently, the annual GPP in 2012 was the lowest. The annual NEE
190 for the four years followed the order of 2015 < 2014 < 2013 < 2012 (Table 4), consistent with the length of the
 CO_2 uptake period.



4 Discussion

4.1 Partitioning the interannual variation in CO₂ exchange

195 The homogeneity-of-slopes model was used to partition the interannual variation (IAV) in CO₂ exchange into climatic variability and ecosystem functional change, which is reflected by the variability of the flux-climate relationship among years (Hui et al., 2003). During the wet season, the daily NEE, GPP and RE were mainly related with T_a (Figure 6). The effect of PAR on NEE and GPP was very weak, with R values of -0.05 and 0.08, respectively.

200 A separate-slopes model was constructed for each year, and the multiple regression model was based on data from the observational period. Compared with the multiple regression model, the separate-slopes model improved the NEE estimation substantially, with R² increasing from 0.69 in the multiple regression model to 0.79 in the separate-slopes model. This means that the separate-slopes model accounted for 10.3% more variation in the observed NEE than the multiple regression model, which is attributed to the functional
205 change (SS_f). The other 89.7% of the variation in the observed NEE was partitioned to interannual climatic variability (SS_i, 7.7%), seasonal climatic variation (SS_s, 37.7%), and random error (SS_e, 44.3%) (Table 5). Therefore, most of IAV in NEE, GPP and RE was attributable to variation in climatic variables, in particular, climatic seasonal variation. This is in line with the findings for a *Skjern* meadow in Denmark and a temperate ombrotrophic bog in Canada (Jensen et al., 2017; Teklemariam et al., 2010). In contrast, Braswell et al. (1997)
210 and Shao et al. (2014) found that functional change accounted for more IAV in fluxes than did direct effects of IAV in climate. Moreover, the contributions of different drivers to the IAV in GPP was similar to that of NEE, while the functional change in RE was twice that of NEE and GPP. The R² for NEE, GPP and RE in the multiple regression model was 0.44, 0.53 and 0.59, respectively. It was reasonable that the random error of NEE was the largest.

215

4.2 Control of the interannual variation in the CO₂ exchange

To examine the interannual variation in CO₂ exchange, the cumulative NEE, GPP and RE in 2013, 2014 and 2015 were compared with those in 2012 (Figure 7). The cumulative NEE_{diff} (the difference in NEE) values for 2014-2012 and 2015-2012 increased rapidly in spring and autumn. In summer, the differences
220 among 2012, 2014 and 2015 varied slightly. Starting in April, the cumulative NEE_{diff} for 2013-2012 increased until early August. These patterns were similar to those for GPP_{diff}. However, the annual cumulative GPP_{diff} (24.3 to 147.2 g C m⁻² yr⁻¹) was relatively larger than the annual cumulative NEE_{diff} (-44.2 to -98.3 g C m⁻² yr⁻¹). The cumulative RE_{diff} decreased from DOY 1 and then increased in spring. The cumulative RE_{diff} for 2013-2012 and 2015-2012 reached its maximum at the end of June, while the cumulative RE_{diff} for
225 2014-2012 increased throughout the entire year, and was the largest.

The daily CO₂ uptake over this meadow ecosystem increases with T_a (Wang et al., 2016). Especially in the



spring (March to May), the temperature environment affected the vegetation growth and GPP. From March to May, the cumulative T_a was 592.3, 577.1, 633.1 and 647.6°C from 2012 to 2015. Consequently, the cumulative GPP in the spring increased in the order 2015, 2014 and 2013. The exception was that the spring of 2012 had higher T_a but lower GPP than the spring of 2013. Compared with the GPP in 2013, the GPP in 2012 increased more significantly due to the higher T_a from March to April. However, the drought in May 2012 delayed vegetation growth and reduced GPP. The difference in GPP_{cum} in 2013-2012, 2014-2012 and 2015-2012 at the end of May was 20.0, 63.1 and 83.3 g C m⁻², representing 82.6%, 42.9% and 59.7% of the difference for the entire year.

From July to October, the NEE, GPP and RE were all strongly correlated with T_a on a monthly scale ($R^2=0.84, 0.86$ and 0.73 , respectively) (Figure 9a, b, c). The slope between GPP and T_a was much larger than that between RE and T_a , indicating that when T_a increased, the alpine meadow ecosystem absorbed more CO₂. The monthly GPP in July and August varied slightly among the four years, while the interannual variability of the GPP in September was the largest because the monthly mean T_a in September for 2012 (8.6°C) and 2013(8.8°C) was significantly lower than those for 2014(9.7°C) and 2015(10.0°C). Consequently, the difference in GPP_{cum} in 2014-2012 and 2015-2012 from September to October was 55.2 and 48.2 g C m⁻², representing 37.5% and 34.6% of the difference for the entire year.

On the annual scale, the annual total NEE decreased (2012, 2013 and 2015) with mean annual T_a (MAT) and then increased when MAT was the highest in 2014. The reason for this was that the annual total RE increased linearly with MAT ($R^2=0.97$), while the relationship between the GPP and MAT was non-linear (Figure 9d). The GPP became saturated with increasing MAT. In contrast, the annual NEE increased with MAT at the Haibei alpine meadow, although the annual NEE was comprehensively controlled by the temperature environment (Kato et al., 2006).

4.3 Comparison of annual CO₂ exchange with other sites

In addition to temperature effects, the daily RE was also correlated with the daily GPP ($RE=0.44GPP+0.63$, $R^2=0.82$) during the wet season from 2012 to 2015. The percentage of RE to GPP for this meadow site was lower than those of Mediterranean grasslands ($RE=0.53GPP+0.72$, $R^2=0.85$, Aires et al., 2008; $RE=0.47GPP+1.33$, $R^2=0.85$, Xu and Baldocchi, 2004).

On the annual scale, the GPP at the study site were much larger than those for semiarid grasslands in Tibet and Canada (Flanagan et al., 2002; Yu et al., 2006), but much lower than the moist grasslands in low-lying areas (Table 7). Due to the high elevation and low soil temperature in the summer, the lower RE caused similar or even lower annual NEE (mean value: -161 g C m⁻² yr⁻¹) at Lijiang than the moist grasslands with low elevation (Table 7). For example, the mean annual NEE for the meadow in Denmark (annual precipitation: 809 mm) was -156 g C m⁻² yr⁻¹, while the mean annual NEE for the C3/C4 grassland in Japan



(annual precipitation: 1156 mm) was $-17 \text{ g C m}^{-2} \text{ yr}^{-1}$. The ratio of RE to GPP ranged from 0.69 to 0.79 over the Lijiang alpine meadow, which was lower than the Haibei alpine meadow (Table 7). This is the reason why the annual NEE of the Lijiang site was on the average 25% lower than the Haibei site. In general, the lower RE/GPP occurred in high-altitude and moist areas. The alpine meadow ecosystem (Lijiang and Haibei) had lower RE/GPP than most of the low-lying grasslands. Compared with semiarid grasslands (RE/GPP: approximately 1.0), the RE/GPP in the moist grasslands was much lower, e. g. the sown grassland in Netherlands (0.60) and the natural grassland in Italy (0.59) (Gilmanov et al., 2007).

5 Conclusions

The 4-year EC data from 2012 to 2015 were used to investigate the interannual variation in the NEE, GPP and RE. The key parameters for ecosystem photosynthesis and respiration were determined for the different seasons of each year. The vegetation growth (NDVI) controlled NEE_{sat} on a monthly scale, and the interannual variation in Q_{10} for the wet and dry seasons was small. The seasonal variation in CO_2 exchange was affected by the seasonal pattern of T_a and the soil moisture in the spring. In the spring, low T_a and drought events delayed the start time of CO_2 uptake. In the late wet season, the higher T_a in 2014 and 2015 resulted in later grass senescence and CO_2 release. The annual NEE decreased with the length of the CO_2 uptake period, but its relationship with the NDVI was not significant. Over this alpine meadow, the HOS model suggests that most of the IAV in NEE, GPP and RE was attributed to seasonal variation in the climatic variables. On an annual scale, the annual RE increased linearly with MAT, while the annual GPP became saturated when MAT increased from 6.16°C to 6.32°C . Thus, the annual NEE decreased and then increased with MAT. The low RE/GPP at the study site was responsible for the lower annual NEE compared with some grassland ecosystem with larger GPP.

Acknowledgements. This study was supported by the National Natural Science Foundation of China (grant No.: 91537212, 41675013, 41661144018, 41461144001, 41305012) and the Third Tibetan Plateau Scientific Experiment: Observations for Boundary Layer and Troposphere (GYHY201406001). The staffs from Lijiang Meteorological Administration are appreciated for their help in the maintenance of the measurements.

References

- Aires, L. M., Pio, C. A., and Pereira, J. S.: Carbon dioxide exchange above a Mediterranean C3/C4 grassland during two climatologically contrasting years, *Glob. Change Biol.*, 14, 539–555, 2008.
- Baldocchi, D.: 'Breathing' of the terrestrial biosphere: lessons learned from a global network of carbon dioxide flux measurement systems, *Aust. J. Bot.*, 56, 1–26, 2008.
- DAHV (Department of Animal Husbandry and Veterinary, Institute of Grasslands, Chinese Academy of Agricultural Sciences), and CISNR (Commission for Integrated Survey of Natural Resources, Chinese Academy of Sciences):



- Rangeland resources of China, China Agricultural Science and Technology, Beijing, 1996.
- Du, Q. and Liu, H. Z.: Seven years of carbon dioxide exchange over a degraded grassland and a cropland with maize ecosystems in a semiarid area of China, *Agr., Ecosyst. Environ.*, 173, 1-12, 2013.
- Falge, E., Baldocchi, D., and Olson, R.: Gap filling strategies for defensible annual sums of net ecosystem exchange, *Agric. For. Meteorol.*, 107, 43-69, 2001.
- 300 Fan, Z.X., Bräuning, A., Thomas, A., Li, J. B., and Cao, K. F.: Spatial and temporal temperature trends on the Yunnan Plateau (Southwest China) during 1961–2004, *Int. J. Climatol.*, 31, 2078–2090, 2011.
- Flanagan, L., Wever, L. A., Carlson, P.: Seasonal and interannual variation in carbon dioxide exchange and carbon balance in a northern temperate grassland, *Glob. Change Biol.*, 8, 599-615, 2002.
- 305 Foken, T. and Wichura, B.: Tools for quality assessment of surface-based flux measurements, *Agric. For. Meteorol.*, 78, 83–105, 1996.
- Fu, Y., Zheng, Z., Yu, G., Hu, Z., Sun, X., Shi, P., Wang, Y., and Zhao, X.: Environmental influences on carbon dioxide fluxes over three grassland ecosystems in China, *Biogeosciences*, 6, 2879–2893, 2009.
- Gilmanov, T. G., Soussana, G. F., Aires, L., Allard, V., Ammann, C., Balzarolo, M., Barcza, Z., Bernhofer, C., Campbell, C. L., and Cernusca, A.: Partitioning European grassland net ecosystem CO₂ exchange into gross primary productivity and ecosystem respiration using light response function analysis, *Agr. Ecosyst. Environ.*, 121, 93-120, 2007.
- 310 Gilmanov, T. G., Aires, L., Barcza, Z., Baron, V. S., Belelli, L., Beringer, J., Billesbach, D., Bonal, D., Bradford, J., Ceschia, E., Cook, D., Corradi, C., Frank, A., Gianelle, D., Gimeno, C., Grünwald, T., Guo, H., Hanan, N., Haszpra, L., Heilman, J., Jacobs, A., Jones, M. B., Johnson, D. A., Kiely, G., Li, S., Magliulo, V., Moors, E., Nagy, Z., Nasyrov, M., Owensby, C., Pinter, K., Pio, C., Reichstein, M., Sanz, M. J., Scott, R., Soussana, J. F., Stoy, P. C., Svejcar, T., Tuba, Z., and Zhou, G.: Productivity, respiration, and light-response parameters of world grassland and agroecosystems derived from flux-tower measurements, *Rangel. Ecol. Manage.*, 63, 16–39, 2010.
- 315 Guo, L. N., He, Z. J., Long, X., Wang, J. Z., Wang, L. D., Li, C. X.: Soil characteristics and its classification system in Mt. Yulong, China, *Guangxi Agric. Sci.*, 40, 1177–1183, 2009, (in Chinese).
- 320 Hui, D., Luo, Y., and Katul, G.: Partitioning interannual variability in net ecosystem exchange between climatic variability and functional change, *Tree Physiol.*, 23, 433–442, 2003.
- Hunt, J. E., Kelliher, F. M., McSeveny, T. M., Ross, D. J., and Whitehead, D.: Long-term carbon exchange in a sparse, seasonally dry tussock grassland, *Glob. Change Biol.*, 10, 1785–1800, 2004.
- Jensen, R., Herbst, M., and Friborg, T.: Direct and indirect controls of the interannual variability in atmospheric CO₂ exchange of three contrasting ecosystems in Denmark, *Agric. For. Meteorol.*, 233, 12-31, 2017.
- 325 Kato, T., Tang, Y. H., Gu, S., Cui, X. Y., Hirota, M., Du, M. Y., Li, Y. N., Zhao, X. Q., and Oikawa, T.: Seasonal patterns of gross primary production and ecosystem respiration in an alpine meadow ecosystem on the Qinghai-Tibetan Plateau, *J. Geophys. Res.*, 109, doi: 10.1029/2003JD003951, 2004.
- Kato, T., Tang, Y. H., Gu, S., Hirota, M., Du, M. Y., Li, Y. N., and Zhao, X. Q.: Temperature and biomass influences on interannual changes in CO₂ exchange in an alpine meadow on the Qinghai-Tibetan Plateau, *Glob. Change Biol.*, 12, 1285-1298, 2006.
- 330 Kormann, R. and Meixner, F. X.: An analytical footprint model for nonneutral stratification, *Bound.-Layer Meteorol.*, 99, 207–224, 2001.



- Liu, J., Zhang, Y., Li, Y., Wang, D., Han, G., and Hou, F.: Overview of grassland and its development in China. Multifunctional grasslands in a changing world volume (I), Guangdong People's Publishing House, Guangzhou, pp. 3–5, 2008.
- Liu, X.D. and Chen, B. D.: Climatic warming in the Tibetan Plateau during recent decades, *Int. J. Climatol.*, 20, 1729–1742, 2000.
- Lloyd, J. and Taylor, J. A.: On the temperature-dependence of soil respiration, *Funct. Ecol.*, 8, 315–323, 1994.
- 340 Moore, C. J.: Frequency response corrections for eddy correlation systems, *Bound.-Layer Meteorol.*, 37, 17–35, 1986.
- Parton, W. J., Scurlock, J. M. O., Ojima, D. S., Schimel, D. S., and Hall, D.O.: Impact of climate change on grassland production and soil carbon worldwide, *Glob. Change Biol.*, 1, 13–22, 1995.
- Polley, H. W., Frank, A. B., Sanabria J., and Phillips, R.: Interannual variability in carbon dioxide fluxes and flux–climate relationships on grazed and ungrazed northern mixed-grass prairie, *Glob. Change Biol.*, 14, 1620–1632, 2008.
- 345 Richardson, A. D., Hollinger, D. Y., Aber, J. D., Ollinger, S. V., and Braswell, B. H.: Environmental variation is directly responsible for short- but not long-term variation in forest atmosphere carbon exchange, *Global. Change Biol.*, 13, 788–803, 2007.
- Shao, J., Zhou, X., He, H., Yu, G., Wang, H., Luo, Y., Chen, J., Gu, L., and Bo, L.: Partitioning climatic and biotic effects on interannual variability of ecosystem carbon exchange in three ecosystems, *Ecosystems*, 17(7), 1186–1201, 2014.
- 350 Shi, P. L., Sun, X. M., and Xu, L. L.: Net ecosystem CO₂ exchange and controlling factors in a steppe-Kobresia meadow on the Tibetan Plateau, *Sci China-Earth Sci*, 49, 207–218, 2006.
- Shimoda, S., Mo, W., and Oikawa, T.: The effects of characteristics of Asian monsoon climate on interannual CO₂ exchange in a humid temperate C3/C4 co-occurred grassland, *SOLA*, 1, 169–172, 2005.
- Suyker, A. E., Verma, S. B., and Burba, G. G.: Interannual variability in net CO₂ exchange of a native tallgrass prairie, *Glob. Change Biol.*, 5, 255–265, 2003.
- 355 Teklemariam, T. A., Lafleur, P. M., Moore, T. R., Roulet, N. T., and Humphreys, E. R.: The direct and indirect effects of inter-annual meteorological variability on ecosystem carbon dioxide exchange at a temperate ombrotrophic bog, *Agric. For. Meteorol.*, 150, 1402–1411, 2010.
- Vickers, D. and Mahrt, L.: Quality control and flux sampling problems for tower and aircraft data, *J. Atmos. Ocean. Technol.*, 14, 512–526, 1997.
- 360 Wang, L., Liu, H. Z., and Bernhofer, C.: Response of carbon dioxide exchange to grazing intensity over typical steppes in a semi-arid area of Inner Mongolia, *Theor. Appl. Climatol.*, DOI 10.1007/s00704-016-1736-7, 2016a.
- Wang, L., Liu, H. Z., Sun, J. H., and Feng, J. W.: Water and carbon dioxide fluxes over an alpine meadow in southwest China and the impact of a spring drought event, *Int. J. Biometeorol.*, 60, 195–205, 2016b.
- 365 Webb, E. K., Pearman, G. I., and Leuning, R.: Correction of flux measurements for density effects due to heat and water vapour transfer, *Q. J. R. Environ. Soc.*, 106, 85–100, 1980.
- Wilczak, J. M., Oncley, S. P., and Stage, S. A.: Sonic anemometer tilt correction algorithms, *Bound-Layer Meteorol.*, 99, 127–150, 2001.
- Xu, L. K. and Baldocchi, D.: Seasonal variation in carbon dioxide exchange over a Mediterranean annual grassland in California, *Agric. For. Meteorol.*, 1232, 79–96, 2004.
- 370 Yu, G. R., Fu, Y., Sun, X., Wen, X., and Zhang, L.: Recent progress and future directions of ChinaFLUX, *Sci China-Earth*



Sci, 49 (Suppl. 1), 1–23, 2006.

Zhao, L., Li, Y., Xu, S. Y., Zhou, H. K., Gu, S., Yu, G. R., and Zhao, X. Q.: Diurnal, seasonal and annual variation in net ecosystem CO₂ exchange of an alpine shrubland on Qinghai-Tibetan plateau, Glob. Change Biol., 12, 1940-195, 2006.

375



Table 1 The average value of daily solar radiation (S_{in} , $\text{MJ m}^{-2} \text{d}^{-1}$), the mean annual air temperature (T_a , $^{\circ}\text{C}$), the mean annual vapor pressure deficit (VPD, kPa), the mean annual soil water content (SWC, $\text{m}^3 \text{m}^{-3}$), the total amounts of precipitation (PPT, mm) for the whole year and the wet season, and the maximum value of NDVI for each year from 2011 to 2015

variables	2012	2013	2014	2015
S_{in}	14.23	14.40	14.44	14.59
T_a	5.93	5.92	6.32	6.16
VPD	0.32	0.30	0.32	0.30
SWC	0.232	0.227	0.232	0.233
PPT (whole year)	1190.4	1066.1	1204.8	1257.4
PPT (wet season)	1086.5	906.1	1092.6	1067.1
NDVI_{\max}	0.60	0.68	0.72	0.72



Table 2 The ecosystem photosynthesis parameters using equation (1) (NEE_{sat} : $\mu\text{mol m}^{-2} \text{s}^{-1}$, α : $\mu\text{mol m}^{-2} \text{s}^{-1}$, R^2) and NDVI for each month during the wet seasons from 2012 to 2015. The regression was based on the average values of $NEE_{daytime}$ and PAR with PAR bins of $100 \mu\text{mol m}^{-2} \text{s}^{-1}$. $NEE_{sat}(a)$ represents the mean value and the standard deviation, $NEE_{sat}(b)$ and $NEE_{sat}(c)$ represent the maximum and minimum values of NEE_{sat} for each month.

Month	NEE_{sat}^a	NEE_{sat}^b	NEE_{sat}^c	α	RE_{bulk}
June	-11.59 ± 2.45	-9.69	-15.08	-0.037 ± 0.009	3.59 ± 0.52
July	-19.67 ± 1.54	-17.46	-21	-0.050 ± 0.009	3.75 ± 0.83
August	-20.14 ± 3.52	-15.43	-23.75	-0.055 ± 0.016	4.15 ± 0.74
September	-16.44 ± 4.56	-11.43	-21.44	-0.051 ± 0.017	3.70 ± 1.04
October	-9.36 ± 1.62	-7.08	-10.9	-0.031 ± 0.005	2.45 ± 0.37

385



Table 3 The ecosystem respiration parameters using equation (2, 3) (a : $\mu\text{mol m}^{-2} \text{s}^{-1}$, b , Q_{10} , R^2) for the wet and dry seasons from 2012 to 2015. The regression was based on the average values of RE and T_{soil} with T_{soil} bins of 1°C

Season	year	a	b	Q_{10}	R^2
Wet season	2012	0.437	0.125	3.48	0.98
	2013	0.374	0.124	3.46	0.94
	2014	0.442	0.126	3.51	0.98
	2015	0.433	0.123	3.43	0.98
Dry season	2012	0.338	0.081	2.25	0.78
	2013	0.202	0.096	2.60	0.74
	2014	0.283	0.115	3.15	0.99
	2015	0.313	0.104	2.82	0.70



Table 4 The annual total NEE, GPP and RE ($\text{g C m}^{-2} \text{ year}^{-1}$) for each year from 2012 to 2015

	2012	2013	2014	2015
NEE	-114.2	-158.5	-159.9	-212.6
GPP	522.3	546.5	669.4	661.8
RE	412.1	393.6	515.2	456.7



395 Table 5 The percentage of the contributions of the seasonal climatic variation (SS_s), interannual climatic variability (SS_i), the ecosystem functional change (SS_f), and random error (SS_e) to the interannual variations in NEE, GPP and RE

	SS_s	SS_i	SS_f	SS_e
NEE	37.7%	7.7%	10.3%	44.3%
GPP	48.6%	9.7%	10.7%	31.0%
RE	48.6%	15.6%	21.2%	14.6%



Table 6 The GPP_{diff} for 2013-2012, 2014-2012 and 2015-2012 during the periods from March to May, June, from June to July, from August to September

Periods	GPP_{diff}		
	2013-2012	2014-2012	2015-2012
March to May	20.0	63.1 (43%)	83.3 (60%)
June	28.7	13.4 (9%)	23.7 (17%)
July to August	-8.7	14.2 (10%)	-18.5 (-13%)
September to October	-12.0	55.2 (38%)	48.2 (35%)
Entire year	24.2	147.1	139.5

400



Table 7 Comparison of mean annual temperature (MAT, °C), mean annual precipitation (MAP, mm yr⁻¹), NEE (g C m⁻² yr⁻¹), GPP, RE and RE/GPP between this study and previous grassland studies

References/ Location	Ecosystem Description	Latitude	Longitude	Altitude	MAT	MAP	NEE	GPP	RE	RE/GPP
This study/ Lijiang, China	Alpine meadow/shrub	27°10'N	100°14'E	3560	6.1	1180	-161 (-213 to -114)	600 (522 to 669)	444 (394 to 515)	0.74 (0.69 to 0.79)
Yu et al., (2006)/ Dauxung, China	Alpine meadow	30°51'N	90°05'E	4250	2.1	520	28 (16 and 39)	167 (144 and 190)	195 (183 and 206)	1.16 (1.08 and 1.27)
Kato et al., (2006)/ Haibei, China	Alpine shrub	37°37'N	101°18'E	3250	-1.0	566	-121 (-193 to -79)	634 (575 to 681)	514 (489 to 556)	0.81 (0.72 to 0.86)
Shimoda et al., (2005)/ Japan	C3/C4 grassland	36°06'N	140°06'E	27	13.9	1156	-17 (-78 to 17)	2365 (2285 to 2426)	2348 (2303 to 2392)	0.99 (0.97 to 1.01)
Aires et al., (2008)/ Portugal	Mediterranean grassland	38°28'N	8°01'E	140	15.5	669	-71 (-190 and 49)	893 (524 and 1261)	822 (573 and 1071)	0.92 (0.85 and 1.09)
Jensen et al., (2017)/ Denmark	Meadow	55°55'N	8°24'E	0	8.7	809	-156 (-356 to -18)	1349 (1147 to 1570)	1193 (1069 to 1406)	0.88 (0.75 to 0.98)
Gilmanov et al., (2007)/ Europe	Multiple (19 sites)	-	-	-0.7 to 1770	3.9 to 14.6	387 to 1816	-150 (-653 to 171)	1261 (467 to 1874)	1111 (493 to 1622)	0.90 (0.59 to 1.14)
Xu and Baldocchi, (2004)/ USA	Mediterranean grassland	38°24'N	120°57'E	129	16.3	559	-52 (-132 and 29)	798 (729 and 867)	747 (735 and 758)	0.94 (0.85 and 1.04)
Flanagan et al., (2002)/ Canada	Temperate grassland	49°26'N	112°34'E	951	-	378	-2 (-21 and 18)	280 (272 and 287)	278 (267 and 290)	1.0 (0.93 and 1.07)

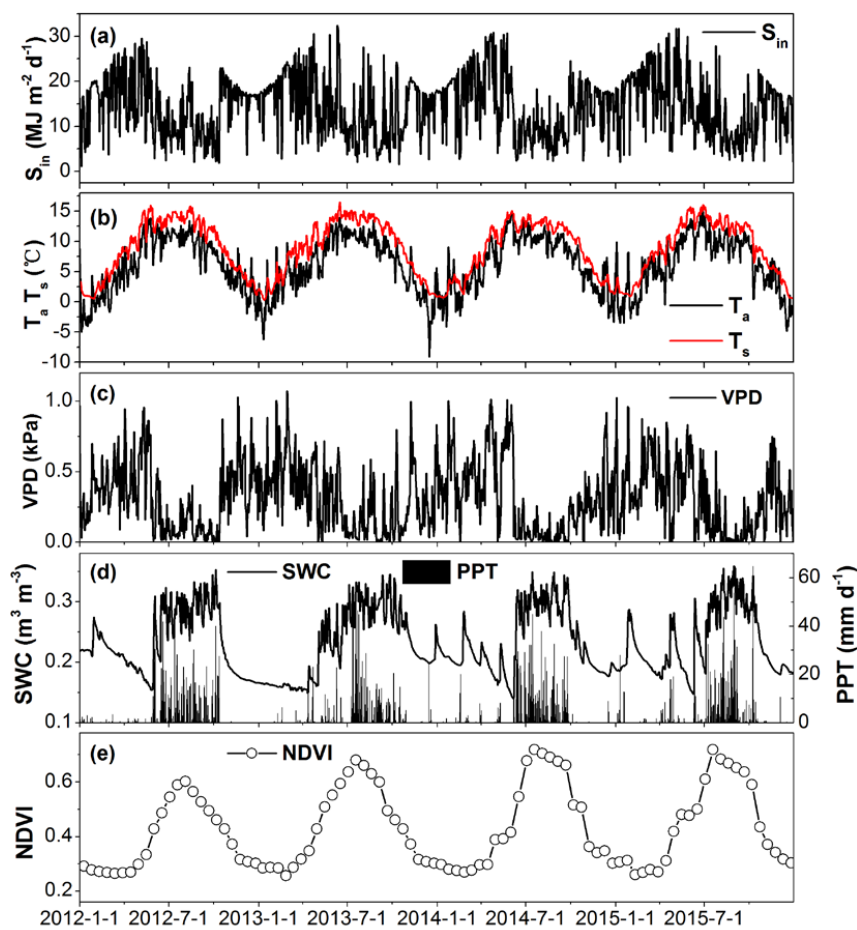


Figure 1 (a) daily sum of solar radiation (S_{in}), daily mean (b) air temperature (T_a), soil temperature (T_s), (c) vapor pressure deficit (VPD, 5 cm) and (d) soil water content (SWC, 5 cm), daily total precipitation (PPT), (e) 16-day average normalized difference vegetation index (NDVI) from 2012 to 2015.

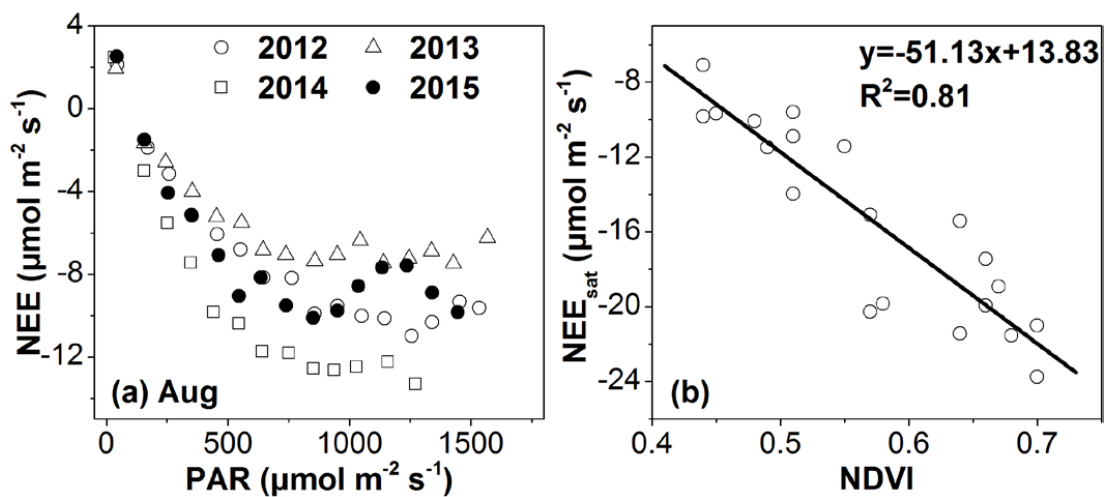


Figure 2 The relationship between daytime NEE and PAR (a) for August from 2012 to 2015. The NEE and PAR data were averaged with PAR bins of $100 \mu\text{mol m}^{-2} \text{s}^{-1}$. (b) the relationship between NEE_{sat} and NDVI on a monthly scale.

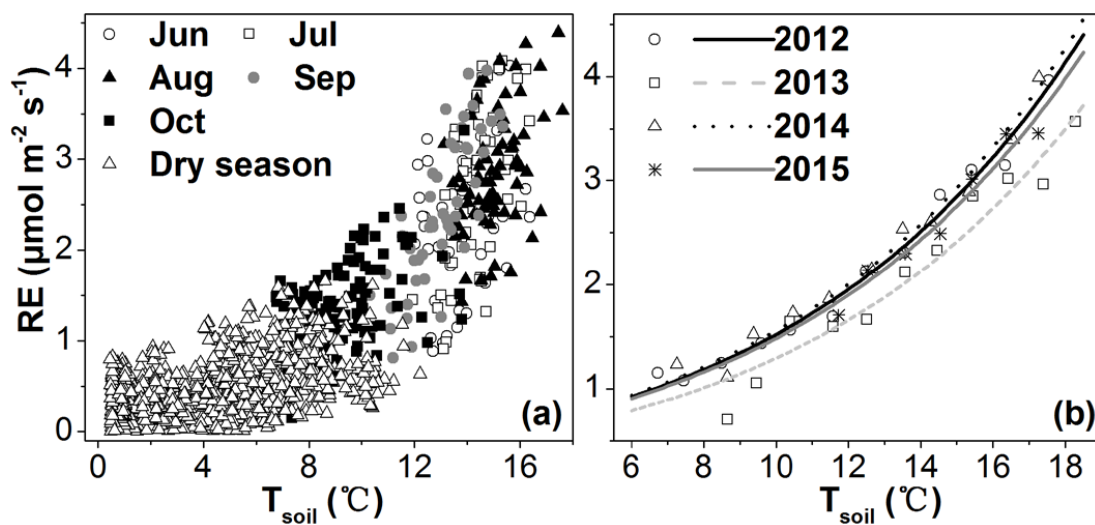


Figure 3 (a) relationship between RE and T_{soil} in 2012; (b) relationship between RE and T_{soil} for the wet season from 2012 to 2015; RE and T_{soil} were averaged with T_{soil} bins of 1 $^{\circ}\text{C}$.

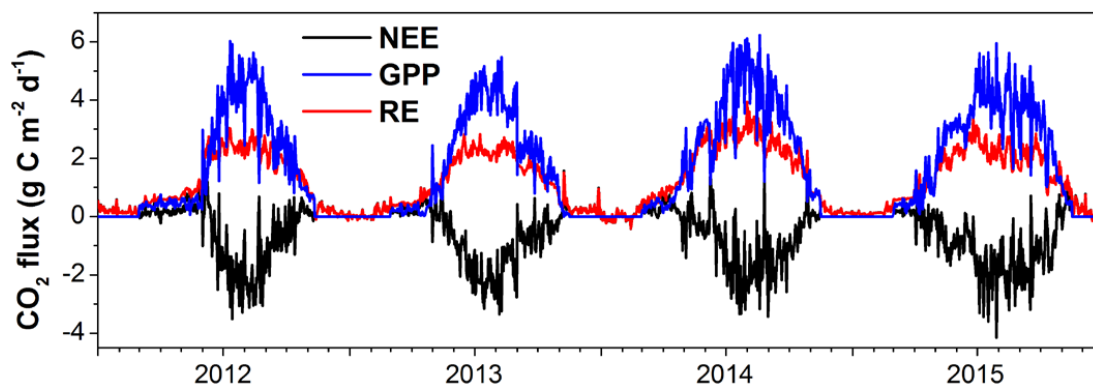


Figure 4 The daily mean NEE, GPP and RE from 2012 to 2015

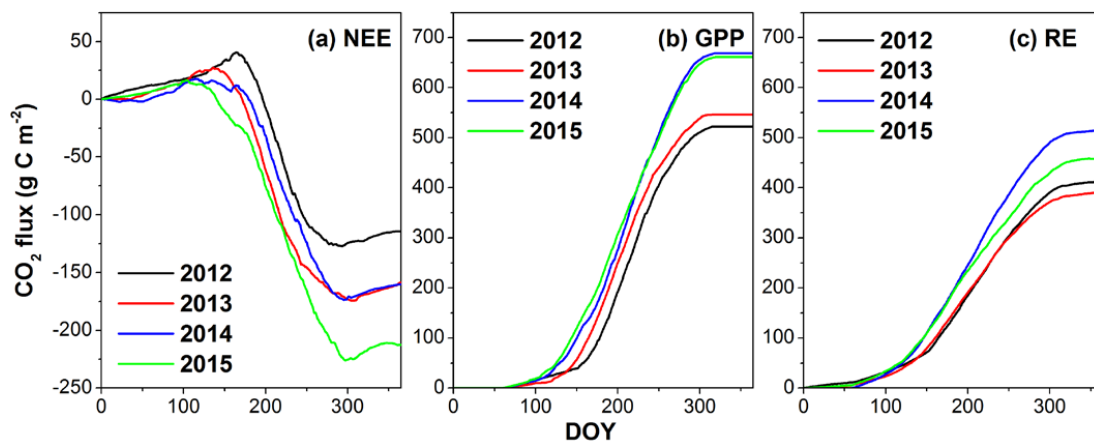


Figure 5 The cumulative NEE, GPP and RE from 2012 to 2015

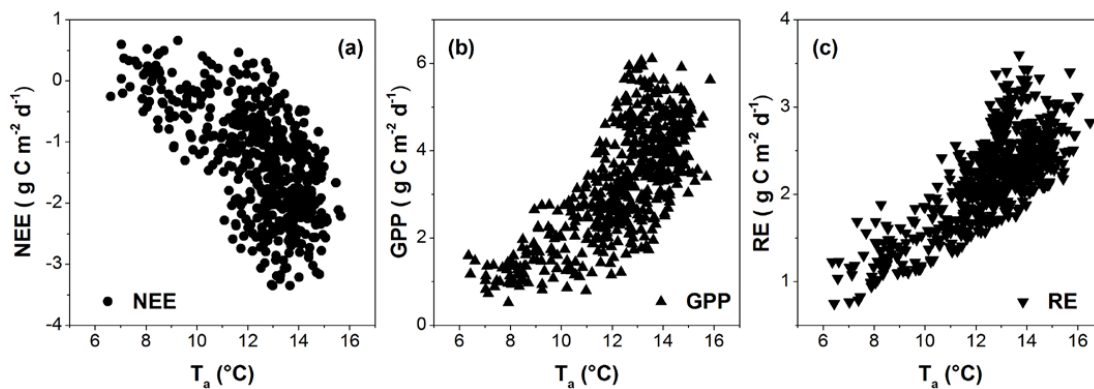


Figure 6 Relationships between (a) NEE and T_a, (b) GPP and T_a, and (c) RE and T_a for the wet seasons from 2012 to 2015

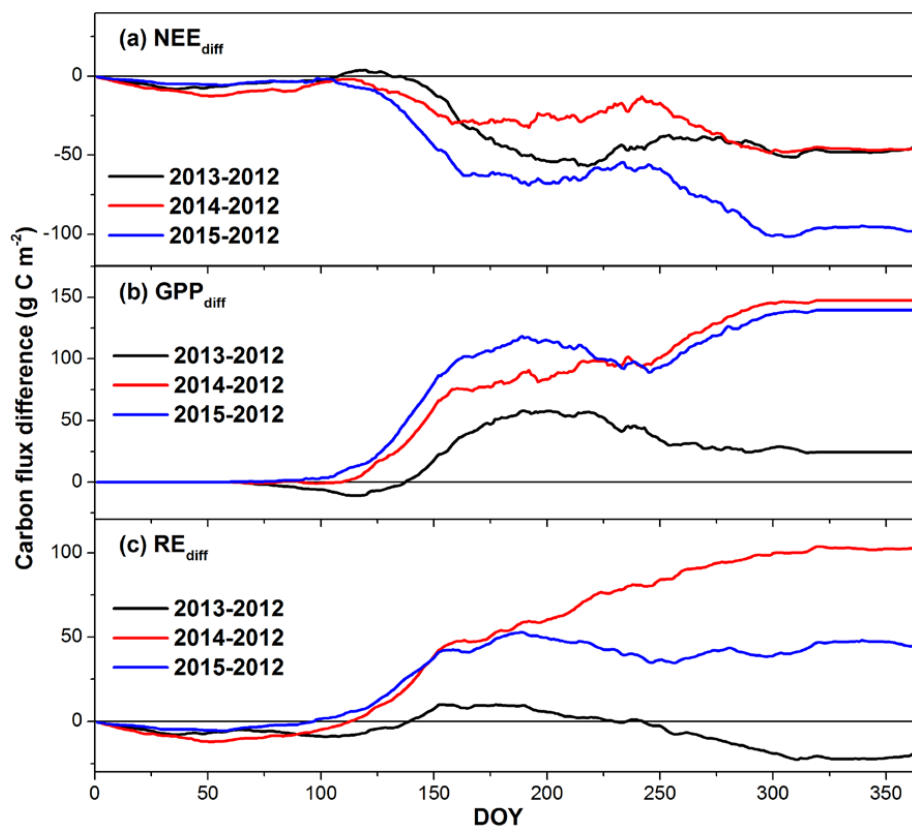


Figure 7 Seasonal variations in the differences of (a) NEE, (b) GPP and (c) RE from 2013 to 2012, from 2014 to 2012 and from 2015 to 2012

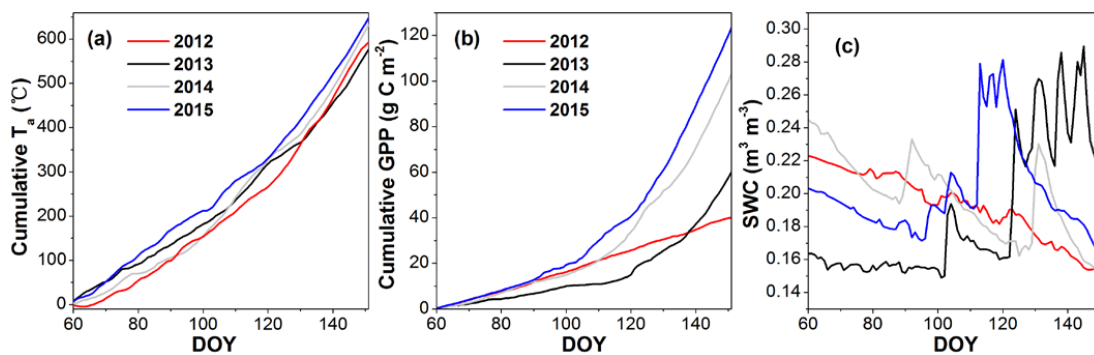


Figure 8 Cumulative (a) T_a and (b) GPP, and (c) the daily mean SWC from March to May (DOY60 to 151) for 2012, 2013, 2014 and 2015

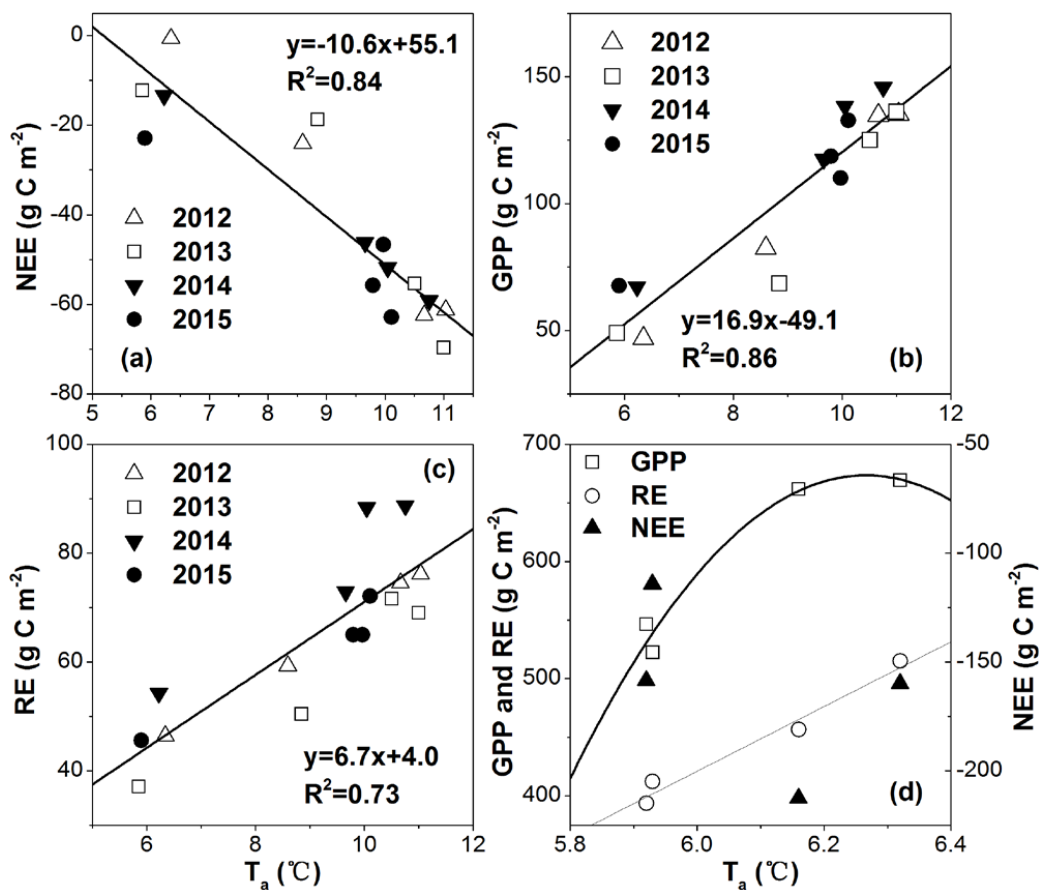


Figure 9 Relationships between (a) NEE and T_a; (b) GPP and T_a; (c) RE and T_s from July to October at a monthly scale, and (d) relationship between the annual total CO₂ exchange fluxes and the mean annual T_a, which were $GPP = -1191T_a^2 + 14930T_a - 46102$, $R^2 = 0.97$, and $RE = 276T_a - 1235$, $R^2 = 0.97$